



## Micro-nano structure poly(ether sulfones)/poly(ethyleneimine) nanofibrous affinity membranes for adsorption of anionic dyes and heavy metal ions in aqueous solution

Minghua Min<sup>a</sup>, Lingdi Shen<sup>a</sup>, Guishan Hong<sup>a</sup>, Meifang Zhu<sup>a</sup>, Yu Zhang<sup>a</sup>, Xuefen Wang<sup>a,\*</sup>, Yanmo Chen<sup>a,\*</sup>, Benjamin S. Hsiao<sup>b</sup>

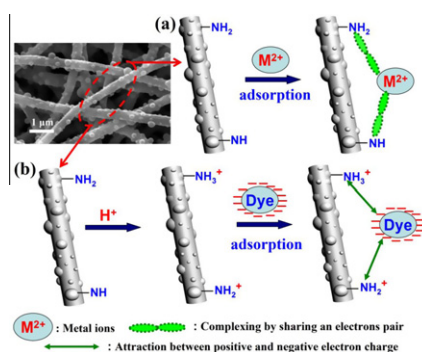
<sup>a</sup> State Key Lab for Modification of Chemical Fibers and Polymer Material, Donghua University, Shanghai 201620, PR China

<sup>b</sup> Department of Chemistry, Stony Brook University, Stony Brook, NY 11794, USA

### HIGHLIGHTS

- ▶ A novel micro-nano structured PES/PEI nanofibrous membrane was fabricated.
- ▶ The adsorption of PES/PEI nanofibrous membranes for metal ions and anionic dyes was tested.
- ▶ Isotherms, kinetic model and thermodynamic parameters were investigated.
- ▶ Two different kinds of adsorption mechanism were proposed for adsorption of anionic and cationic compounds.
- ▶ The regeneration efficiency of PES/PEI nanofibrous membranes was studied.

### GRAPHICAL ABSTRACT



### ARTICLE INFO

#### Article history:

Received 11 February 2012

Received in revised form 3 May 2012

Accepted 5 May 2012

Available online 15 May 2012

#### Keywords:

Adsorption

Poly(ethyleneimine)

Heavy metal ions

Anionic dyes

Micro-nano structure

### ABSTRACT

In this study, a novel micro-nano structure poly(ether sulfones)/poly(ethyleneimine) (PES/PEI) nanofibrous membrane was fabricated and utilized as an adsorbent for anionic dyes or heavy metal ions from aqueous solutions. A series of adsorption experiments were carried out to investigate the influence of membrane dosage, initial solution pH value, contact time, initial solution concentration and adsorption temperature on the adsorption performance. The experimental results showed that the removal of the anionic dyes and metal ions on this PES/PEI nanofibrous membrane was a pH-dependent process with the maximum adsorption capacity at the initial solution pH of 1 for anionic dyes and 5–7 for metal ions, respectively, and the PES/PEI nanofibrous membranes could be regenerated successfully. The adsorption equilibrium data were all fitted well to the Langmuir isotherm equation, with a maximum adsorption capacity values of 1000.00 mg/g, 344.83 mg/g, 454.44 mg/g, 94.34 mg/g, 161.29 mg/g and 357.14 mg/g for Sunset Yellow FCF, Fast Green FCF, Amaranth, Pb(II), Cu(II) and Cd(II), respectively. The kinetic study indicated that the adsorption of metal ions and anionic dyes could be well fitted by the pseudo-second-order equation, suggesting the intra-particle diffusion process as the rate-limiting step of the adsorption process. Thermodynamic parameters such as free energy, enthalpy and entropy of adsorption of anionic dyes and metal ions were also evaluated and the results showed that the adsorption was a spontaneous physical adsorption process. In addition, two different kinds of adsorption mechanism were proposed to explain the adsorption of anionic and cationic compounds on the PES/PEI nanofibrous membrane.

Crown Copyright © 2012 Published by Elsevier B.V. All rights reserved.

\* Corresponding authors. Tel.: +86 21 67792860; fax: +86 21 67792855.

E-mail addresses: [wangxf@dhu.edu.cn](mailto:wangxf@dhu.edu.cn) (X. Wang), [ymc@dhu.edu.cn](mailto:ymc@dhu.edu.cn) (Y. Chen).

## 1. Introduction

The removal of heavy metal pollutants and dyes from wastewater has become a critical issue because of their adverse effects on human health and the environment [1,2]. Adsorption has been proved to be a well-established and economical method for the treatment of wastewater contaminated by metal ions and dyes. Nowadays, almost all the adsorbents developed for the removal of heavy metal ions and dyes rely on the interaction of the target compounds with the functional groups that are present on the surfaces of the adsorbents [1]. Therefore, a large surface area and many adsorption sites of the matrix are essential for adsorption affinity membranes to remove the contaminants from wastewater, and the specific surface area was one of the most important factors to affect the adsorption capacity of the adsorbents [3–5]. Electrospinning technology for the preparation of nanofibers or nanostructure materials is one of the most important objects in the recent research topics. In addition, the nanofibers or nanostructure materials fabricated by electrospinning have been widely used as affinity nanofibrous membranes [6–9], because of their superior properties such as fine diameters, large specific surface area, high porosity, small inter-fibrous pore size and stability in liquid media [10,11].

In the adsorption process, the functional groups such as amino and carboxyl groups on the surface of the adsorbents played an important role in determining the effectiveness, capacity, selectivity, and reusability of the adsorbent materials [12–14]. Further more, adsorbents with amino groups showed bifunctional properties which enable them to adsorb cationic and anionic target compounds at different pH values in aqueous solutions [1]. Neutral nitrogen of amine group with a lone pair electrons have been found to be one of the most efficient functional groups for the removal of heavy metal ions [15,16], and protonic amino groups with a cationic charge can adsorb anionic pollutants by means of electrostatic attraction [1,17].

Polyethyleneimine (PEI), with a large amount of amino and imino groups in its polymer chain, has been widely investigated not only as an immobilization material for sensors [18–21], but also as a chelating agent for heavy metal ions removal [22–25]. Based on our preliminary work [26], a novel micro-nano structure nanofibrous affinity membranes of poly(ether sulfones) (PES) blended with PEI were fabricated by electrospinning technique followed by solvent etching in crosslinking solution. Primary investigation for the removal of copper ion was performed, indicating that this micro-nano structure nanofibrous affinity membrane owned potential application in affinity membranes.

The aim of this work is to investigate the adsorption capabilities and mechanism of the micro-nano structure PES/PEI nanofibrous membrane for the removal of heavy metal ions (that is Pb(II), Cu(II) and Cd(II), respectively) and three anionic dyes, namely Sunset Yellow FCF (SY FCF), Fast Green FCF (FG FCF) and Amaranth (AM), from aqueous solutions. The effects of various operating parameters including membrane dosage, initial solution pH value, contact time, initial solution concentration, solution temperature, and recycling efficiency of this micro-nano structure PES/PEI nanofibrous affinity membrane were thoroughly investigated. Various kinetic and equilibrium models for the adsorption of these target ions and molecules on the micro-nano structure PES/PEI nanofibrous membrane were also discussed.

## 2. Materials and methods

### 2.1. Materials

Branched polyethyleneimine (PEI) ( $M_w = 60,000$  g/mol) in 50% (w/v) aqueous solution was purchased from Sigma–Aldrich and

concentrated under vacuum at 40 °C to obtain 80% (w/v) PEI aqueous solution for further application. Poly (ether sulfones) (PES) ( $M_w = 64,000$  g/mol) was kindly supplied by Shanghai Solvay Co., Ltd., China. The preparation process of the micro-nano structure PES/PEI nanofibrous membrane could be found in our previous work [26]. N,N-dimethylacetamide (DMAc), glutaraldehyde (GA) (25% aqueous solution), acetone, sodium hydroxide (NaOH), ethylenediaminetetraacetic acid (EDTA),  $Pb(NO_3)_2$  ( $M_w = 331.21$  g/mol),  $Cu(NO_3)_2 \cdot 3H_2O$  ( $M_w = 241.60$  g/mol),  $Cd(NO_3)_2 \cdot 4H_2O$  ( $M_w = 308.48$  g/mol), Sunset Yellow FCF (SY FCF), Fast Green FCF (FG FCF) and Amaranth (AM) were purchased from Shanghai Chemical Reagent Plant and used as received. The characteristics and structures of the dyes are summarized in Table 1.

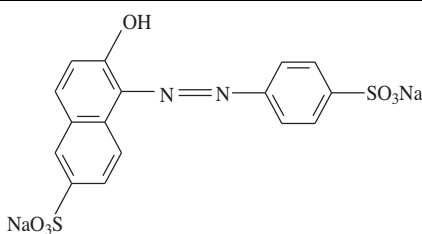
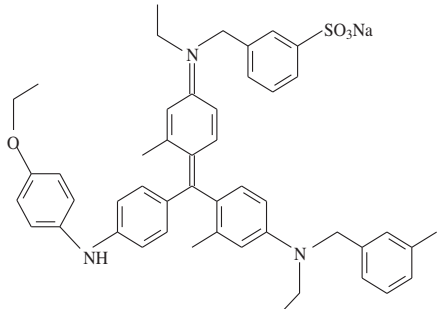
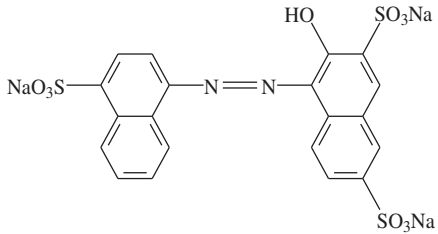
### 2.2. Preparation of micro-nano structure PES/PEI nanofibrous membranes

The detailed preparation procedure of micro-nano structure PES/PEI nanofibrous membranes was shown in our previous work [26]. Firstly, PEI was concentrated under vacuum at 40 °C to obtain 80% (w/v) PEI aqueous solution. Secondly, PES was dissolved in DMAc at 50 °C for 8 h until it became a homogeneous solution. And then, PES solution and PEI solution were mixed together at 30 wt.% total polymer concentration, and a solution with PEI/PES blend ratio of 1:1.4 was used for the electrospinning experiment. Typical parameters for electrospinning experiments were as follows [26]: the applied electric voltage was 18 kV, the solution feed rate was 2.2  $\mu$ l/min, and the distance between the spinneret and the collector (a grounded metallic drum) was 15 cm. The grounded rotating metallic drum with diameter of 10 cm and length of 30 cm was used to collect the deposited nanofibers at a rotating speed of 180 rpm. Finally, the electrospun PES/PEI nanofiber scaffold was immersed in GA/water/acetone solution for 2 h. In this solution, PEI was not only solvent etched by solvent water but also simultaneously crosslinked by GA. The GA crosslinking solutions were prepared by mixing water and acetone at weight ratio of 70/30, and a given amount of GA was then added into the water/acetone mixture and 0.5 M HCl solution was used to adjust the pH value of the solution to 4.0.

### 2.3. Measurements of micro-nano structure PES/PEI nanofibrous membranes

The morphology of the electrospun PES/PEI nanofibrous membrane was examined by scanning electron microscopy (SEM) (JSM-5600LV, Japan). The average diameter of the nanofibers in the experiment was measured from the SEM image using image analysis software. The Brunauer–Emmett–Teller (BET) surface area, pore volume and pore width of the micro-nano structure PES/PEI nanofibrous membrane were characterized by using  $N_2$  adsorption–desorption isotherms with a surface area analyzer (ASAP 2010, micromeritics Co., USA). FT-IR spectrum was obtained in attenuated total reflectance (ATR) mode using a Nicolet 8700 FT-IR spectrometer (USA) with a resolution of 4  $cm^{-1}$ , in the range of 4000–750  $cm^{-1}$ . Thermal analysis was performed with a NET-ZSCH TG 209 F1 (Germany). The test was conducted under air purge (20 mL/min) with sample weights of about 5 mg over a temperature range of 30–900 °C at heating rate of 10 °C/min. The X-ray photoelectron spectroscopy (XPS) measurements were made on a Kratos Axis Ultra<sup>DLD</sup> spectrometer (Kratos Analytical-A Shimadzu Group Company) with monochromatic Al K $\alpha$  radiation as the excitation and an X-ray power of 75 W. Survey scans were taken from 0 to 1200 eV binding energies, using both electrostatic and magnetic lenses, with a 40 eV pass energy, a step size of 0.5 eV, and dwell time of 100 ms. Elemental peaks were fit using CasaXPS software

**Table 1**  
Characteristics and structures of the anionic dyes used in this study.

Generic name	Abbreviation	M.W.	$\lambda_{\max}$ (nm)	Molecular structure
Sunset Yellow FCF	SY FCF	452.38	482	
Fast Green FCF	FG FCF	808.85	624	
Amaranth	AM	604.47	521	

(Casa Software Ltd., Teignmouth, Devon, UK). Component peak shapes were fitted using a Gaussian–Lorentzian model.

#### 2.4. Adsorption experiments

Adsorption of SY FCF, FG FCF, AM, Pb(II), Cu(II) and Cd(II) from aqueous solutions was investigated in a series of static adsorption experiments. All adsorption experiments were carried out by using 50 mL of metal ion and dyes solutions of different initial concentrations for different adsorbent dosages. Effects of pH (1.0–7.0), kinetic experiments (0–24 h), adsorption isotherm (initial concentration 50–1500 mg/L for heavy metal ions, and 100–2000 mg/L for anionic dyes), and thermodynamic studies (278–323 K) on adsorption were studied. All the adsorption isotherm experiments were carried out at temperature of 303 K. The membranes were kept in solution mounted on a horizontal shaking table (100 rpm) for 24 h to ensure complete equilibration [25].

The samples of heavy metal ions and the anionic dyes solutions in the course of adsorption were collected at regular intervals of time. And the concentrations of the heavy metal ions and the anionic dyes solutions were determined by inductively coupled plasma/optical emission spectrometry (ICP–OES, Prodigy, USA) and UV–vis spectrophotometer (Lambda 35, PerkinElmer, USA), respectively. The amount of adsorbates adsorbed on the PES/PEI nanofibrous membranes was calculated according to the following equation:

$$q_e = \frac{(C_0 - C_e) \cdot V}{m} \quad (1)$$

where  $C_0$  and  $C_e$  are the initial and equilibrium adsorbates concentrations ( $\text{mg L}^{-1}$ ), respectively.  $V$  is the volume of the solution (L) and the  $m$  is the weight of the membrane used (mg).

The heavy metal ions and the anionic dyes removal percentage can be calculated according to below equation:

$$\text{Removal percentage} = \frac{C_0 - C_e}{C_0} \times 100\% \quad (2)$$

#### 2.5. Desorption experiments

The experiments for desorption efficiency were carried out with 0.05 M EDTA and 0.05 M NaOH solutions for heavy metal ions and the anionic dyes, respectively. The micro-nano structure PES/PEI nanofibrous membranes were first equilibrated with heavy metal ions or the anionic dyes in aqueous solutions with an initial concentration of 400 mg/L then put into the desorption solution. Desorption was allowed for a time period up to 24 h. After the desorption test, the membranes were washed with deionized water, and reused in the next cycle of adsorption experiment. The adsorption–desorption experiments were conducted for three cycles. The desorption efficiency ( $De$ ) was determined from the following equation:

$$De = \frac{C \times V}{q \times m} \times 100\% \quad (3)$$

where  $C$  (mg/L) is the concentration of adsorbates in the desorption solution,  $V$  is the volume of the desorption solution,  $q$  (mg/g) is the

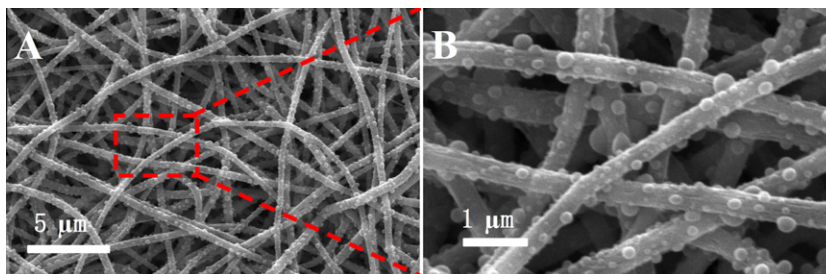


Fig. 1. Typical SEM images of the micro-nano structure PES/PEI nanofibrous membranes (A: magnification 5000 $\times$ ; B: magnification 20,000 $\times$ ).

amount of adsorbates adsorbed on the PES/PEI nanofibrous membranes before desorption experiment, and  $m$  (mg) is the amount of the adsorbent used in the desorption experiments.

### 3. Results and discussion

#### 3.1. Micro-nano structure PES/PEI nanofibrous membranes

The typical SEM images were shown in Fig. 1. It was found that the average diameter of the micro-nano structure PES/PEI nanofibers was about 350 nm, and the average size of the spherules onto the nanofibers was about 200 nm, respectively. The formation of micro-nano structural surface of the nanofibrous membranes was caused by the crosslinking of PEI in crosslinking solution accompanied by solvent etching due to the solvation between viscous PEI and the solvent water. In our previous work, it was found when the water content was low (<20%), the rate of PEI crosslinking by GA was relatively fast, and the content of solvent etched PEI on the fiber surface by water was low. PEI was crosslinked and formed a layer with very small spherules on the fiber surface. When the water content was increased (~30%), the rate of solvent etching of PEI by water increased and more etched PEI near fiber surface was crosslinked and coagulated to form larger size spherules and deposited on the surface of nanofibers. However, when the water content was increased further (>40%), PEI was dissolved and diffused fast into the crosslinking solution, and the deposited nano-scale PEI spherules decreased and became smaller. The content of solvent water in crosslinking solution was a critical factor for the morphology of the resulting nanofibers. PES was inert in the crosslinking system, so the fiber framework was integrated. Furthermore, the micro-nano structure was also observed in the interior of the crosslinked PES/PEI nanofibrous membrane [26]. This unique morphology could bring much more surface area per unit mass, indicating that this micro-nano structure material could be extended easily to the huge potential application in affinity membranes and nanosensors.

The chemical structures of the micro-nano structure PES/PEI nanofibrous membrane were analyzed with an FT-IR spectrometer and the IR spectrum was shown in Fig. 2. The vibration absorption of C–H bond at 2930  $\text{cm}^{-1}$  and 2820  $\text{cm}^{-1}$  was appeared. The characteristic absorption band around 1650  $\text{cm}^{-1}$  could be assigned to the absorption peaks of the C=O stretching of carbonyl groups because the GA was used as the crosslinking agent [22]. Besides, the vibration absorption at 1486  $\text{cm}^{-1}$  and 1579  $\text{cm}^{-1}$  were ascribed to the stretching vibration absorption of C–N–H or C=N bond [27]. The appearances of these bands revealed that the macromolecular chains of PEI have chemically linked onto the surfaces of the micro-nano structure PES/PEI nanofibrous membrane. The peak at 1243  $\text{cm}^{-1}$  was due to the anti-symmetric C–O–C stretching of the aryl ether group. The peak found at 1323  $\text{cm}^{-1}$  and 1296  $\text{cm}^{-1}$  doublet resulting from anti-symmetric O=S=O stretching of the sulfone group and that at 1152  $\text{cm}^{-1}$  was due to the

symmetric O=S=O stretching of sulfone group, which were characteristic band for PES [28].

Thermo-gravimetric curve of the micro-nano structure PES/PEI nanofibrous affinity membranes is very much in agreement with other results. From Fig. 3, it was found that the decomposition process included three sections. The part one was attributed to evaporation of water adsorbed on the surface of the PES/PEI nanofibrous membranes, because of the strong hydrogen bond between the amine and imino groups of PEI and water molecules in the ambient air. When the temperature was about 200  $^{\circ}\text{C}$ , the mass loss was likely due to decomposition of the amine groups on the PEI macromolecules chains [27,29]. And then the decomposition of the PEI component was accelerated at a higher temperature (<500  $^{\circ}\text{C}$ ) because its backbone was attacked by the decomposed

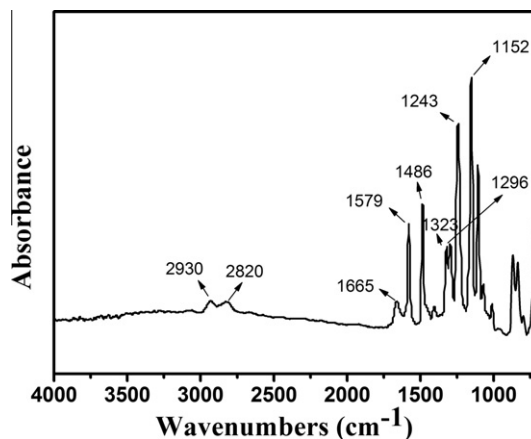


Fig. 2. IR spectrum of the micro-nano structure PES/PEI nanofibrous membrane.

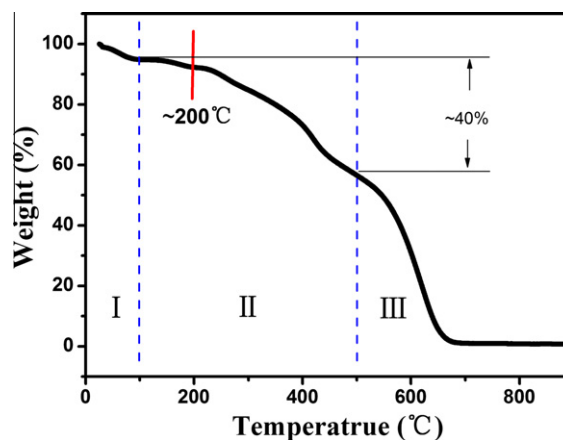


Fig. 3. Thermo-gravimetric curve of the micro-nano structure PES/PEI nanofibrous membranes.



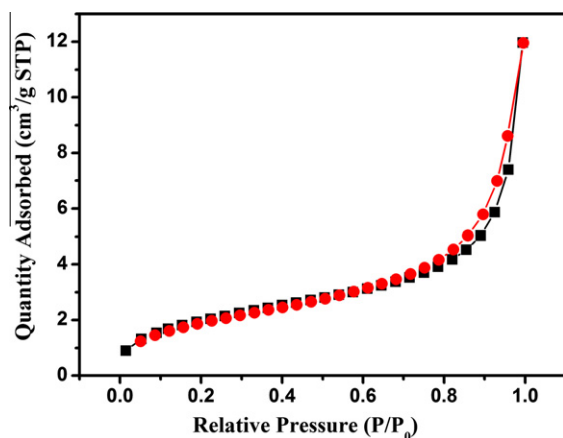


Fig. 4. Nitrogen adsorption–desorption isotherm of the micro-nano structure PES/PEI nanofibrous membrane.

amine groups during the deamination reaction [30]. When the temperature was increased further (about 500 °C), the decomposition of PES component was beginning [31], and the mass loss was about 40%. As the temperature reached beyond around 680 °C, the mass of the membranes tended to be stable, indicating the decomposition of the PES/PEI nanofibrous membranes was complete. It can be concluded that the micro-nano structure PES/PEI nanofibrous membranes showed good thermal stability.

The results of the BET analysis of the micro-nano structure PES/PEI nanofibrous membrane were shown in Fig. 4. It can be assigned as a type II isotherm, which was attributed to physical adsorption and also indicating a high affinity between gas and solid [32]. Benefiting from the micro-nano structure, the specific surface area of the PES/PEI nanofibrous membrane was 7.27 m<sup>2</sup>/g, and higher than which composed of smooth nanofibrous [33]. The large specific surface area and porous structure indicated the PES/PEI nanofibrous membrane have huge potential application in the adsorption separation.

### 3.2. Effect of membrane dosage

The membrane dosage is an important parameter in adsorption studies because it determines the capacity of adsorbent for a given initial concentration of adsorbate solution. To study the dosage effect of the micro-nano structured PES/PEI nanofibrous membranes on heavy metal ions and the anionic dyes adsorption, experiments were conducted at initial metal ion/dye concentration of 100 mg/L (pH 5), while the amount of PES/PEI nanofibrous membranes added was varied. Fig. 5 shows the effect of membrane dosage on the percentage removal of the anionic dyes and heavy metal ions. It was observed that the percentage removal of the SY FCF, FG FCF and AM dyes rapidly increased with the increase of membranes dosage up to 0.8 g/L, 1.2 g/L and 0.8 g/L, respectively, and thereafter remained invariant (Fig. 5a). However, the percentage removal of heavy metal ions rapidly increased with the increase in membrane dose up to 2 g/L, and thereafter remained unchanged (Fig. 5b). At equilibrium time, the maximum percentage removal for SY FCF, FG FCF, AM, Pb(II), Cu(II) and Cd(II) was 99.89%, 99.95% and 99.33%, 90.43%, 89.81% and 93.18%, respectively. The percentage removal increase at lower membrane dosage was due to the increase in the available sorption sites on the surface of PES/PEI nanofibers in the membrane.

### 3.3. Effect of solution pH

Solution pH had a significant effect on the uptake of dyes, since it determines the surface charge of the adsorbent and the degree of

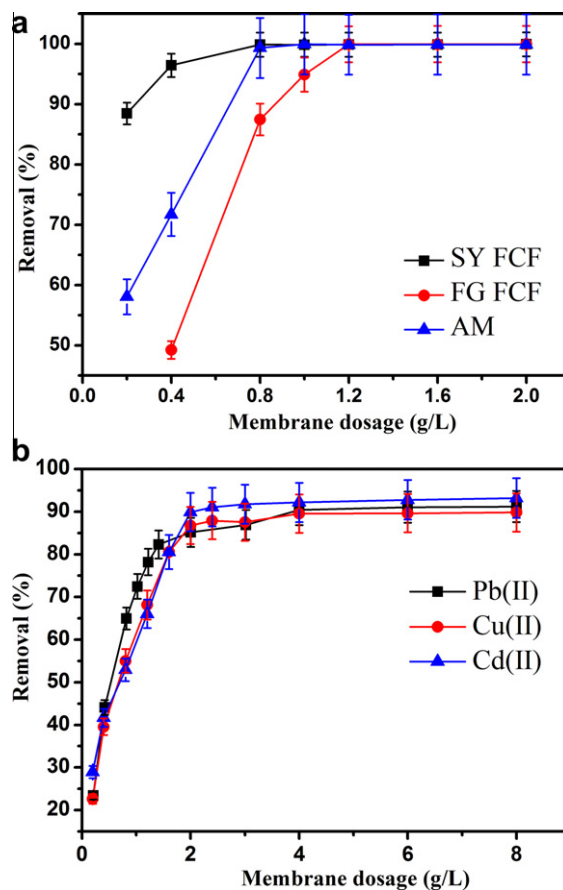


Fig. 5. Effect of membrane dosage on the percentage removal of the anionic dyes (a) and three heavy metal ions (b).

ionization and speciation of the adsorbates [34]. The amine and imino groups ( $-\text{NH}_2$  and  $-\text{NH}-$ ) on PEI will be protonated to form  $-\text{NH}_3^+$  and  $-\text{NH}_2^+$  depending on the pH value of the solution. The amine forms of  $-\text{NH}_3^+$ ,  $-\text{NH}_2^+$  will attract anions [35]. Fig. 6 showed the relationship between the initial solution pH and contaminants removal. The results revealed that the adsorption behavior of micro-nano structure PES/PEI nanofibrous membranes with heavy metal ions and the anionic dyes was strongly pH-dependent. It was found that the adsorption capacity of the anionic dyes decreased with solution pH increase from 1 to 7 (Fig. 6a), but for heavy metal ions, the adsorption capacity increased with pH increase from 1 to 7 (Fig. 6b).

At low pH solution, a relatively high concentration of protons would be available to protonate amine and imino groups of PEI chain to form  $-\text{NH}_3^+$  and  $-\text{NH}_2^+$  groups, which will compete strongly with heavy metal ions for amine sites. On the other hand, protonated amine and imino groups will increase strong electrostatic attractions between negatively charged dye anions and positively charged adsorption sites, resulting in an increased adsorption of dyes. Furthermore, the protonation of amine groups would lead to strong electrostatic repulsion of the heavy metal ions to be adsorbed. As a result, it became difficult for heavy metal ions to come into close contact with the adsorbent surface and be adsorbed on it [36]. However, at higher solution pH values of 5–7 (lower proton concentrations), as regards to the anionic dyes, less protons would be available to protonate  $-\text{NH}_2$  and  $-\text{NH}-$  to form  $-\text{NH}_3^+$  and  $-\text{NH}_2^+$  groups, respectively, consequently decrease the electrostatic attractions between negatively charged dye anions and adsorbent surface. On the other hand, as regards to the heavy metal ions, the competition between protons and heavy metal ions

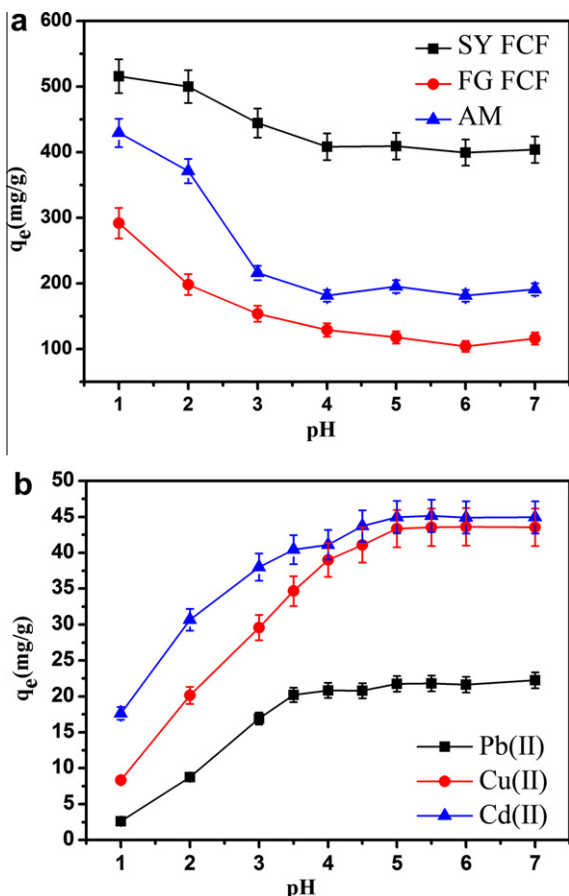


Fig. 6. Effect of solution pH values on the adsorption of the anionic dyes (a) and heavy metal ions (b) on PES/PEI nanofibrous membranes.

for the amine groups became less significant, and more of the amine groups existed in their neutral form, which reduced the electrostatic repulsion of heavy metal ions. Furthermore, the unpaired electrons of the amine groups could also create coordinate bonds with the heavy metal ions. More heavy metal ions would be adsorbed onto the surfaces of the PES/PEI nanofibrous membranes, resulting in the increase of adsorption capacity of the heavy metal ions at higher pH values.

It can be seen that the pH of aqueous solution plays an important role in the adsorption of heavy metal ions and anionic dyes onto PES/PEI nanofibrous membranes. The optimum pH values for heavy metal ions and the anionic dyes adsorption were found to be in the pH range of 5–7 and 1, respectively, and all further adsorption experiments were carried out at solution pH of 5 for heavy metal ions, and pH of 1 for the dyes.

#### 3.4. Effect of the initial concentration

Fig. 7 showed the effect of the initial concentration on the adsorption capacity of the PES/PEI nanofibrous membranes. The results showed that the adsorption capacity of the three anionic dyes and three heavy metal ions increases with increasing initial concentrations and then tends to level off. The increase of the adsorption capacity of PES/PEI nanofibrous membranes can be attributed to the increase in the driving force of concentration gradient with an increase in the initial concentration [37]. Finally the complexes between the chelating sites and the absorbates reached saturation. When the initial absorbate concentration was 2000 mg/L, the maximum absorption capacity for SY FCF, FG FCF, AM, Pb(II), Cu(II) and

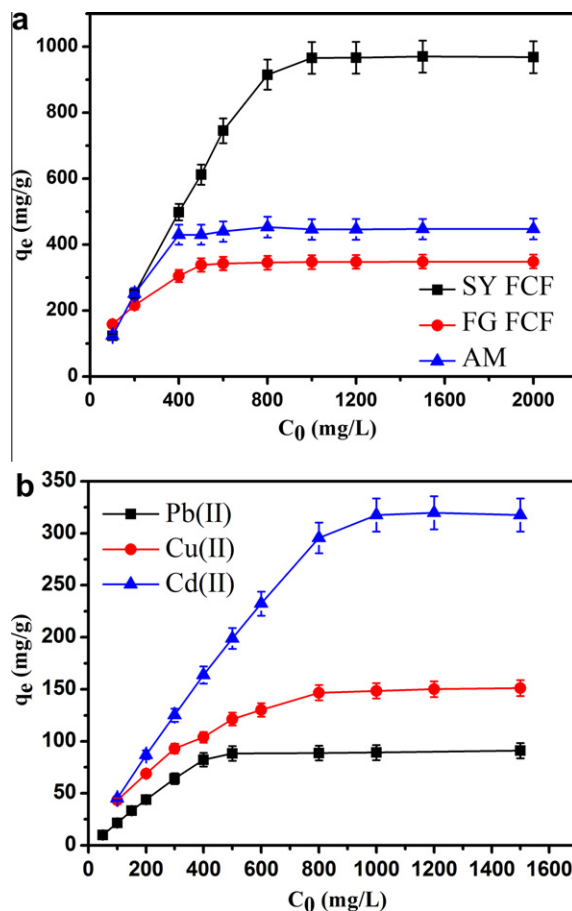


Fig. 7. Effect of the initial concentration on the adsorption of the anionic dyes (a) and heavy metal ions (b) on PES/PEI nanofibrous membranes.

Cd(II) were 968.31 mg/g, 348.03 mg/g, 447.38 mg/g, 90.06 mg/g, 151.17 mg/g and 317.59 mg/g, respectively.

In order to prove the outstanding effect of PEI component in PES/PEI nanofibrous affinity membranes, the pure PES nanofibrous membrane was also used for removal the anionic dyes and heavy metal ions. It was found that when the initial absorbate concentration was 1000 mg/L, the maximum absorption capacity of pure PES nanofibrous membranes for SY FCF, FG FCF, AM, Pb(II), Cu(II) and Cd(II) were 4.19 mg/g, 3.30 mg/g, 3.06 mg/g, 1.02 mg/g, 0.16 mg/g and 0.75 mg/g, respectively. These results indicated the adsorption amounts of pure PES nanofibrous membranes were very low and the PES mainly functioned as a matrix.

#### 3.5. Effect of contact time

The effect of contact time for the adsorption of the three anionic dyes and heavy metal ions on PES/PEI nanofibrous membrane was studied for a period of 24 h, as shown in Fig. 8. It was found that the adsorption capacity of anionic dyes and heavy metal ions improved with increased contact time. However, the adsorption processes become saturated after 10 h for SY FCF, 14 h for FG FCF, 14 h for AM, 5 h for Pb(II), 5 h for Cu(II) and 3 h for Cd(II), respectively, indicating that the adsorption of heavy metal ions was much faster than the adsorption of the anionic dyes.

#### 3.6. Effect of temperature

The effect of temperature on adsorption of the anionic dyes and heavy metal ions was studied in the temperature range of

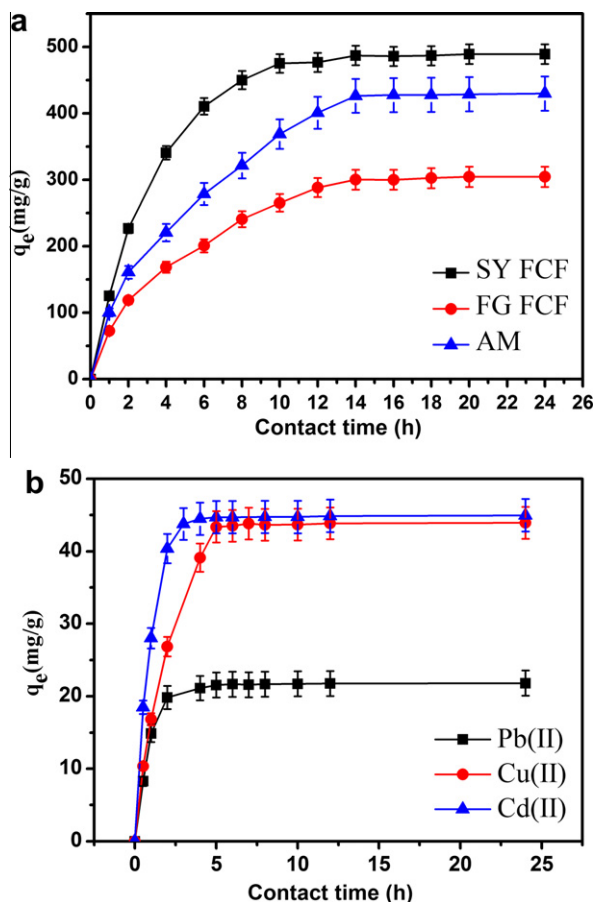


Fig. 8. Effect of contact time on the adsorption of the anionic dyes (a) and heavy metal ions (b) on PES/PEI nanofibrous membranes.

278–323 K, and the results were shown in Fig. 9. It was found that the adsorption capacity of the three anionic dyes increased with the temperature increase (Fig. 9a), indicating an endothermic nature of the adsorption process of the anionic dyes onto the PES/PEI nanofibrous membrane. However, the adsorption capacity of heavy metal ions decreased with increasing temperature (Fig. 9b), which indicated that the adsorption of heavy metal ions were exothermic process. Further, adsorption of heavy metal ions was favored at lower temperature. Similar results were found for heavy metal ions adsorption onto amidoximated bacterial cellulose [38].

### 3.7. Adsorption isotherms

Adsorption isotherms indicate how the adsorbates (heavy metal ions or anionic dyes) interact with adsorbents and how adsorption uptakes vary with adsorbate concentrations at given pH values and temperatures. In this study, two well-known models of Langmuir and Freundlich isotherms were used to analyze the results of the equilibrium isotherms, and the correlation coefficient ( $R^2$ ) was calculated to evaluate the fit of the two models.

The Langmuir adsorption model is based on the assumption that the maximum adsorption corresponds to a saturated monolayer of adsorbate molecules on the adsorbent surface. Thus, adsorption occurs uniformly on the active sites of the adsorbent, and once an adsorbate occupies a site, no further adsorption will take place at this site [36]. The widely used Langmuir isotherm has been found to be useful in many real adsorption processes and the adsorption data is analyzed according to the Langmuir isotherm equation as follow [39]:

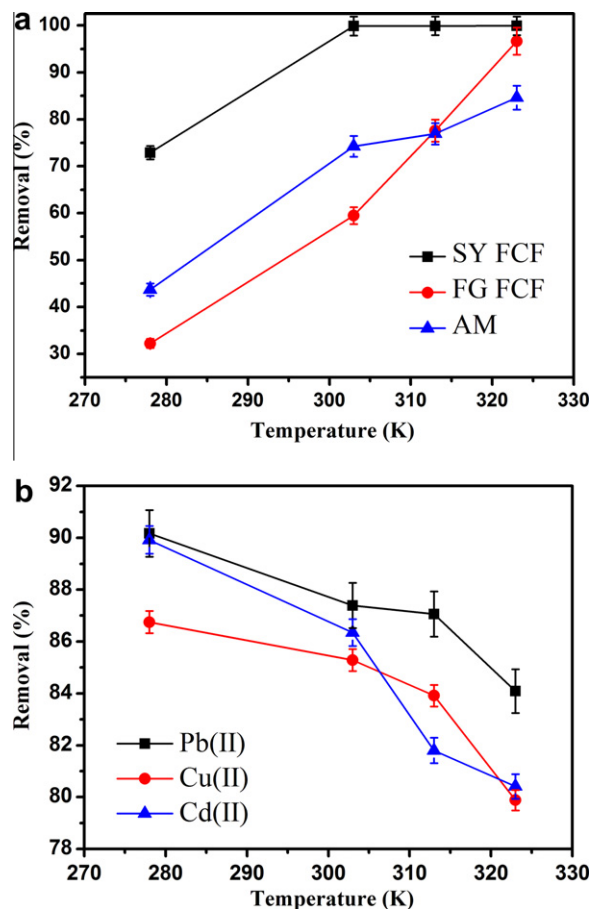


Fig. 9. Effect of temperature on the adsorption of the anionic dyes (a) and heavy metal ions (b) on PES/PEI nanofibrous membranes.

$$\frac{C_e}{q_e} = \frac{C_e}{q_0} + \frac{1}{bq_0} \quad (4)$$

where  $q_e$  is the amount of adsorbate adsorbed on the membrane at adsorption equilibrium (mg/g),  $C_e$  is the equilibrium adsorbate concentration in solution ( $\text{mg L}^{-1}$ ),  $q_0$  represents the maximum uptake of the adsorbate (mg/g) and  $b$  is the Langmuir constant ( $\text{L/mg}$ ), related to the binding energy of adsorption (affinity), respectively. A plot of  $C_e/q_e$  versus  $C_e$  yields a straight line with a slope of  $1/q_0$  and intercept of  $1/bq_0$  (Fig. 10). According to the slope and

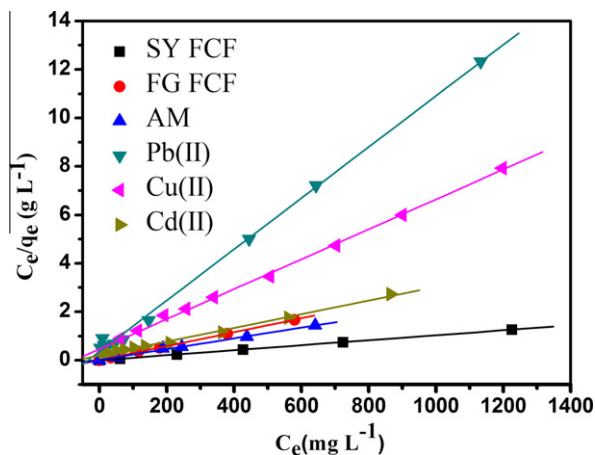
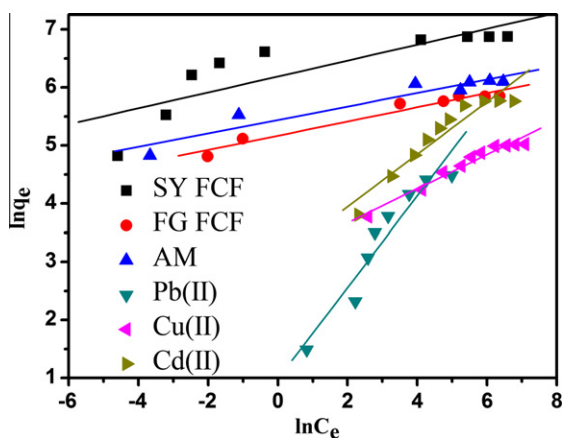


Fig. 10. Adsorption isotherms of the anionic dyes and heavy metal ions on PES/PEI nanofibrous membranes according to the Langmuir equation.

**Table 2**

Langmuir and Freundlich constants for the adsorption of the anionic dyes and heavy metal ions on PES/PEI nanofibrous membranes.

Target compound	Langmuir constants			Freundlich constants		
	$q_0$ (mg/g)	$b$ (L/mg)	$R^2$	$K_F$ (mg/g)	$n$	$R^2$
SY FCF	1000.00	1.1111	0.9999	485.99	7.31	0.7019
FG FCF	344.83	0.3085	0.9997	175.23	8.17	0.9570
AM	454.55	0.1618	0.9975	230.19	8.67	0.9066
Pb(II)	94.34	0.0295	0.9974	2.67	1.27	0.9197
Cu(II)	161.29	0.0134	0.9974	21.78	3.41	0.9621
Cd(II)	357.14	0.0140	0.9953	20.89	2.21	0.9110

**Fig. 11.** Adsorption isotherms of the anionic dyes and heavy metal ions on PES/PEI nanofibrous membranes according to the Freundlich equation.

intercept of the fitted line, the value of  $q_0$  and  $b$  can be estimated, as shown in Table 2. The value of the correlation coefficient  $R^2$  for the Langmuir equation was 0.9999, 0.9997, 0.9975, 0.9974, 0.9974 and 0.9953 for SY FCF, FG FCF, AM, Pb(II), Cu(II) and Cd(II), respectively, which suggested that the adsorption of the three heavy metal ions and anionic dyes on the PES/PEI nanofibrous membranes followed the Langmuir adsorption isotherm. And the maximum adsorption capacities (from Langmuir isotherm data) for SY FCF, FG FCF, AM, Pb(II), Cu(II) and Cd(II) were 1000.00 mg/g, 344.83 mg/g, 454.44 mg/g, 94.34 mg/g, 161.29 mg/g and 357.14 mg/g, respectively.

The well-known Freundlich isotherm is an empirical equation employed to describe the heterogeneous systems. The linear form of a Freundlich equation can be represented as follows [40]:

$$\ln q_e = \ln K_F + \frac{\ln C_e}{n} \quad (5)$$

where  $K_F$  is the constant depicting adsorption capacity related to bond strength and the slope  $1/n$  is a measure of the adsorption intensity or surface heterogeneity. The value of  $K_F$  and  $n$  can be determined from the linear plot of  $\ln q_e$  versus  $\ln C_e$  (Fig. 11). From Table 2, the  $n$  values (1.27–8.67) were in range of  $n > 1$  for the anionic dyes and heavy metal ions, revealing the favorable adsorption.

It was found that the value of the correlation coefficient  $R^2$  of the three heavy metal ions and the anionic dyes estimated from the Langmuir equation was significantly higher than that estimated from Freundlich equation (Table 2), indicating that the Langmuir equation gives a better fit to the experimental data than the Freundlich equation.

### 3.8. Adsorption kinetics

Adsorption kinetic data are often analyzed using two commonly used kinetic models, namely, the pseudo-first-order [41], the

pseudo-second-order [42] and an intraparticle diffusion [43,44] kinetic models, which can be expressed in their linear forms as Eqs. (6)–(8), respectively:

$$\ln(q_e - q_t) = \ln q_e - k_1 t \quad (6)$$

The plot of  $\ln(q_e - q_t)$  versus  $t$  gives a straight line with a slope of  $-k_1$  and an intercept of  $\ln q_e$ .

$$\frac{t}{q_t} = \frac{1}{k_2 q_e^2} + \frac{t}{q_e} \quad (7)$$

The plot of  $t/q_t$  versus  $t$  gives a straight line with a slope of  $1/q_e$  and an intercept of  $1/(k_2 q_e^2)$ .

$$q_t = K_p t^{1/2} + C \quad (8)$$

The plot of  $q_t$  versus  $t^{1/2}$  gives a straight line with a slope of  $K_p$  and an intercept of  $C$ .

The adsorption kinetic plots for the adsorption of anionic dyes and heavy metal ions were shown in Fig. 12 and all the obtained kinetic parameters were summarized in Table 3. The results (the correlation coefficients  $R^2$  listed in Table 3) clearly indicated that the adsorption kinetics closely followed the pseudo-second-order kinetic model rather than the pseudo-first-order kinetic model, suggesting that intra-particle diffusion process was the rate-controlling step of the adsorption process [45]. So it is necessary to analyze the intraparticle diffusion model, which can describe the adsorption process more clearly. Since this was a solid-liquid adsorption process, the adsorbate transfer was characterized by either boundary layer diffusion and intraparticle diffusion, or a combination of both [43]. This possibility was explored using the intraparticle diffusion model [43,44]. Some authors have reported that it is essential for the plots to cross the origin if the intraparticle diffusion is the sole rate-controlling step [46]. In this work, the plot does not pass through the origin, instead, two linear portions were obtained (Fig. 12c). These results indicate that two or more steps occur in the adsorption processes, involving instantaneous adsorption on the external surface, intraparticle diffusion or gradual adsorption being the rate-controlling stage, and the final equilibrium stage where the intraparticle diffusion slows down due to the extremely low solute concentration in solution [46]. Phase I corresponds to the actual intraparticle diffusion, including adsorption on the macro-pores and meso-pores of the PES/PEI nanofibrous membrane, until the exterior surface reached the saturation [47]. Phase II corresponds to the equilibrium stage. The data showed that the diffusion in macro-pores and meso-pores was significant, indicating the intra-particle diffusion was the real rate-controlling step of the adsorption process.

### 3.9. Adsorption thermodynamics

The adsorption of the anionic dyes and heavy metal ions on the PES/PEI nanofibrous membrane was studied at temperature range of 298–323 K to determine the thermodynamic parameters, from which the changes in standard enthalpy ( $\Delta H^0$ ), standard entropy



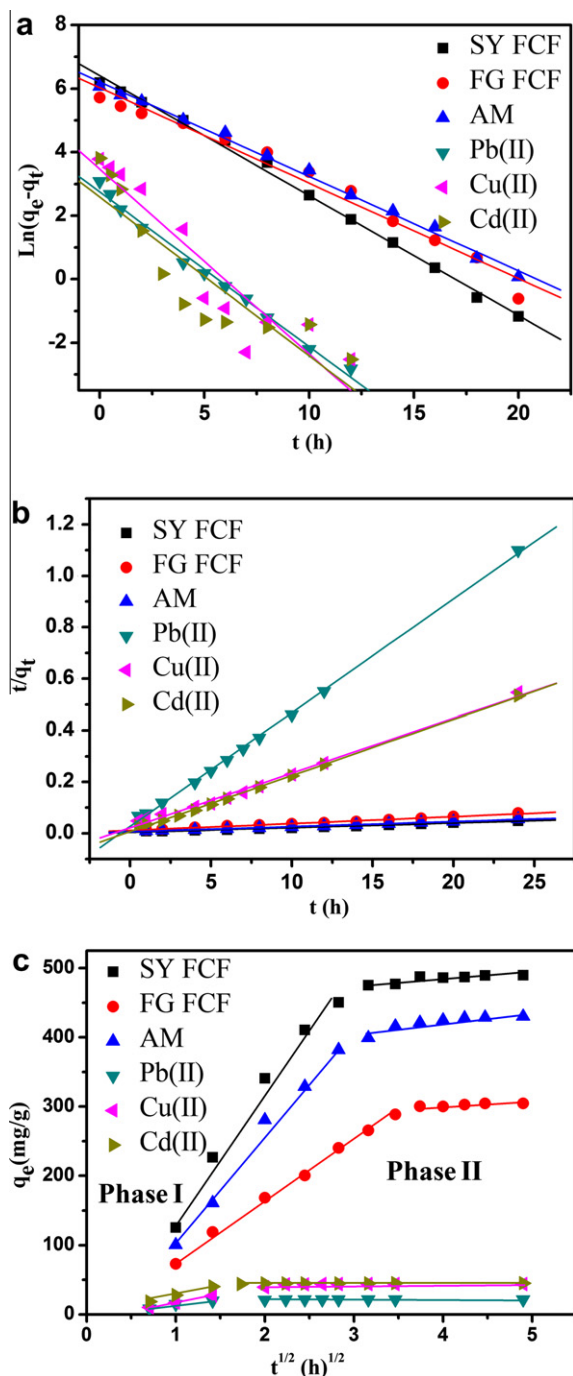


Fig. 12. Pseudo-first-order kinetic model (a), pseudo-second-order kinetic model (b) and intraparticle diffusion model (c) for the adsorption of the anionic dyes and heavy metal ions on PES/PEI nanofibrous membranes.

Table 3  
Adsorption kinetic parameters for the adsorption of the anionic dyes and heavy metal ions on PES/PEI nanofibrous membranes.

Absorbates	Pseudo-first-order model			Pseudo-second-order model			Intraparticle diffusion model			
	$k_1$ ( $\text{h}^{-1}$ )	$q_e$ (mg/g)	$R^2$	$k_2$ ( $\text{g}/(\text{mg h}^{-1})$ )	$q_e$ (mg/g)	$R^2$	$k_{p1}$ ( $\text{mg}/(\text{g h}^{-1})$ )	$R_{p1}^2$	$k_{p2}$ ( $\text{mg}/(\text{g h}^{-1})$ )	$R_{p2}^2$
SY FCF	0.3771	604.92	0.9921	0.000736	555.56	0.9944	178.41	0.9831	9.59	0.9672
FG FCF	0.3004	414.51	0.9777	0.000639	370.37	0.9935	86.56	0.9973	6.29	0.8884
AM	0.2977	499.89	0.9948	0.000606	500.00	0.9931	143.82	0.9788	9.22	0.9054
Pb(II)	0.4894	8.47	0.8792	0.0734	22.62	0.9990	16.03	0.9861	2.46	0.9242
Cu(II)	0.5819	32.16	0.8747	0.0210	46.95	0.9931	23.37	0.9994	3.68	0.9628
Cd(II)	0.4999	13.32	0.7960	0.0689	45.87	0.9990	25.34	0.9669	3.96	0.9468

( $\Delta S^0$ ), and standard free energy ( $\Delta G^0$ ) due to the transfer of unit mole of solute from solution onto the solid–liquid interface can be obtained. The values of  $\Delta H^0$  and  $\Delta S^0$  were calculated using the following equations [48]:

$$\Delta G^0 = -RT \ln K_d \quad (9)$$

$$\Delta G^0 = \Delta H^0 - T\Delta S^0 \quad (10)$$

where  $R$  (8.314 J/mol K) is the universal gas constant,  $T$  (K) is the absolute solution temperature, and distribution adsorption coefficient,  $K_d$ , is calculated from the following equation:

$$K_d = \frac{C_0 - C_e}{C_e} \cdot \frac{V}{m} \quad (11)$$

where  $C_0$  is the initial concentration (mg/L),  $C_e$  is the equilibration concentration after adsorption (mg/L),  $V$  is the volume of the solution (L), and  $m$  is the dose of the membrane (g). From Eqs. (9) and (10), the van't Hoff equation was obtained as:

$$\ln K_d = \frac{\Delta S^0}{R} - \frac{\Delta H^0}{RT} \quad (12)$$

As shown in Fig. 13, the plot of  $\ln K_d$  versus  $1/T$  gives a straight line with a slope of  $\Delta H^0$  (kJ/mol) and an intercept of  $\Delta S^0$  (kJ/mol K). The values of these thermodynamic parameters (measured at different temperatures) are listed in Table 4.

The negative free energy changes ( $\Delta G^0$ ) at all the studied temperatures suggested that the adsorption of the anionic dyes and heavy metal ions onto PES/PEI nanofibrous membrane was thermodynamically feasible and spontaneous. This reveals an increased randomness at the solid–solution interface during the fixation of the dyes on the active sites of the nanofibrous membrane. The positive value of  $\Delta H^0$  further indicated that the adsorption of anionic dyes was an endothermic in nature, and the adsorption capacity increased with increasing temperature. The negative values of  $\Delta G^0$  decreased with increasing temperature as shown in Table 4 suggested the favorable and spontaneous adsorption process of anionic dyes on the nanofibrous membrane. The positive values of  $\Delta S^0$  indicated the increased randomness at the solid/solution interface during the adsorption of dyes in aqueous solution on the nanofibrous membrane. However, for the adsorption of heavy metal ions, the negative value of  $\Delta H^0$  indicated that the adsorption process was exothermic process. This was explained that the adsorption capacity of heavy metal ions decreased with increasing temperature.

Furthermore, some researchers have reported that physical sorption energies are in the range of 0 to  $-20$  kJ/mol and chemisorption energies in the range of  $-80$  to  $-400$  kJ/mol [12]. Therefore, the interaction between the absorbates and PES/PEI nanofibrous membrane can be considered as a physical adsorption rather than chemisorption.

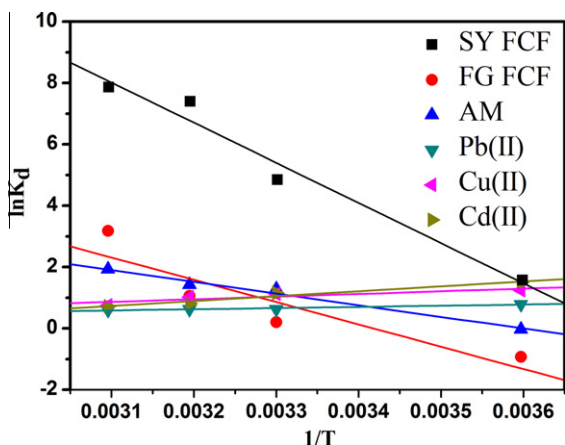


Fig. 13. Plot of  $\ln K_d$  versus  $1/T$  for the estimation of thermodynamic parameters.

### 3.10. Adsorption mechanism

As discussed in the literature, the main adsorption sites for the anionic dyes and heavy metal ions are amino and imino groups on the PEI macromolecular chains which have bifunctional properties that enabled them to adsorb cationic and anionic target compounds at different pH values in aqueous solutions [1]. It is necessary to investigate the amount and state of amino and imino groups which was distributed on the surface of the PES/PEI nanofibrous membrane. The surface property of the PES/PEI nanofibrous membranes before and after adsorption was characterized by XPS. XPS spectra given in Fig. 14 were measured over a wide binding energy region to survey for all the elements present on the surface of the membranes. For the virgin PES/PEI nanofibrous membrane, the appearance of a binding energy (BE) peak from the N 1s at  $\sim 399$  eV and the XPS data of N 1s on the PES/PEI nanofibrous membrane before adsorption were shown in Fig. 14a. It was found that the

content of the N atoms in the membrane surface was 7.39%. In addition, the amount of three kinds of amino groups (amino group, imino group and tertiary amino group) was 33.32%, 53.29%, and 13.39%, respectively. The BE peaks at 165.8 eV and 167 eV are assigned to S 2p, which suggested the presence of PES on membrane surface [49]. In addition, based on the content of N 1s and S 2p, the mass ratio of PEI/PES was estimated roughly, which was about 1:1.28. This ratio was a little higher than that ratio (1:1.4) in the spinning solution, indicating that PEI concentrated and formed a layer with very small spherules on the fiber surface at the nanofiber surface during the process of crosslinking accompanied by solvent etching due to the solvation between viscous PEI and the solvent water.

For the heavy metal ions, there were some characteristic BE peaks appeared after adsorption (Fig. 14b–d). The peaks at the BE of 934.1 eV, 137.9 eV and 404.8 eV were attributed to the Cu 2p orbital, Pb 4f orbital and Cd 3d orbital, respectively. Therefore, these BE peaks provide evidence of Cu(II), Pb(II) and Cd(II) being adsorbed on the PES/PEI nanofibrous membrane [50,51]. After heavy metal ions adsorbed, the BE peak of N 1s around at 398.9 eV changed into two BE peaks around at 397.4 eV and 404.0 eV, indicating that the nitrogen of amine and imino group had a lone pair of electrons which could bind a metal ion. However, for the adsorption of anionic dyes, the BE peak of N 1s around at 398.9 eV moved to 396.5 eV (Fig. 14e–g), which indicated the electrostatic interaction between the PES/PEI nanofibrous membrane and the anionic dyes [52].

As reported above, a possible adsorption mechanism between target compounds and bifunctional amino and imino groups on the polymer PEI chains has been proposed as shown in Fig. 15. At low solution pH values, a relatively high concentration of protons was available to protonate amine and imino groups of PEI chain to form  $-\text{NH}_3^+$  and  $-\text{NH}_2^+$  groups, resulting in an increase in the anionic dyes adsorption. On the other hand, the protonation of amine groups leads to strong electrostatic repulsion of the cationic metal ions to be adsorbed. However, at higher solution pH values of 5–7 (lower proton concentrations), less protons would be available to protonate  $-\text{NH}_2$  and  $-\text{NH}-$  to form  $-\text{NH}_3^+$  and  $-\text{NH}_2^+$  groups, neutral nitrogen of amine and imino group have a lone pair of electrons which can bind a metal ion through sharing an electron pair to form a metal complex [53,54]. As a result, metal ions are thus more favorably adsorbed onto the surfaces of the PES/PEI nanofibrous membranes at relative higher pH values.

Table 4  
Thermodynamic parameters for the adsorption of the anionic dyes and heavy metal ions on PES/PEI nanofibrous membranes at different temperature.

Target compound	Temperature (K)	$\Delta G^0$ (kJ/mol)	$\Delta H^0$ (kJ/mol)	$\Delta S^0$ (kJ/mol K)
SY FCF	278	-4.06	108.99	0.4039
	303	-14.51		
	313	-18.70		
	323	-22.88		
FG FCF	278	3.01	60.50	0.2068
	303	-2.16		
	313	-4.23		
	323	-6.30		
AM	278	-0.02	31.76	0.1143
	303	-2.87		
	313	-4.02		
	323	-5.16		
Pb(II)	278	-1.82	-2.90	-0.0039
	303	-1.72		
	313	-1.68		
	323	-1.64		
Cu(II)	278	-6.79	-7.21	-0.0015
	303	-7.76		
	313	-6.74		
	323	-6.73		
Cd(II)	278	-12.31	-13.28	-0.0035
	303	-12.22		
	313	-12.18		
	323	-12.15		

### 3.11. Desorption and repeated use

Good desorption performance of an adsorbent is an important factor necessary for its potential practical application. In our previous study [22], it was found that the PEI nanofibrous affinity membrane adsorbed with heavy metal ions could be regenerated successfully in 0.05 M EDTA aqueous solution without significantly affecting its adsorption efficiency. In addition, Lin [1] reported that 0.05 M NaOH was an effective regeneration solution for the desorption of the anionic dyes. In this study, 0.05 M EDTA and 0.05 M NaOH were chosen for the desorption of heavy metal ions and the anionic dyes, respectively. The results of the desorption efficiency for heavy metal ions and the anionic dyes were shown in Table 5. For heavy metal ions, it was found that the desorption efficiency reached 96.2% even after the third cycles. This result was comparable with our previous study, and suggested that the adsorption ability of PES/PEI nanofibrous membranes was kept at a high level after several repetitions of the adsorption–desorption cycles. However, for the desorption of anionic dyes, the adsorption efficiency was deteriorated to 99.8% for SY FCF, 90.6% for FG FCF, and 72.2% for AM, respectively, even after the first cycle. After three cycles, desorption efficiency of SY FCF and FG FCF was kept

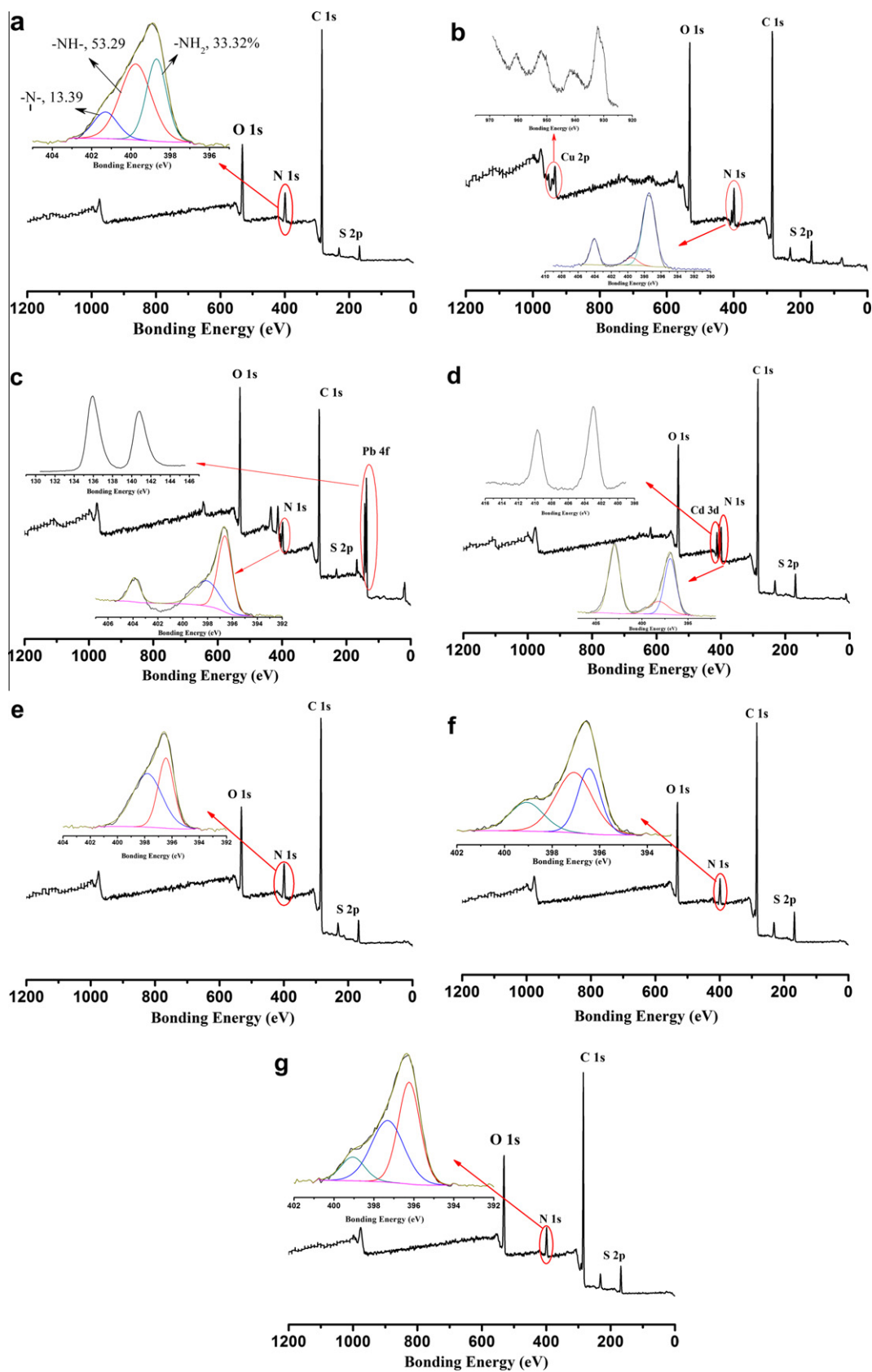
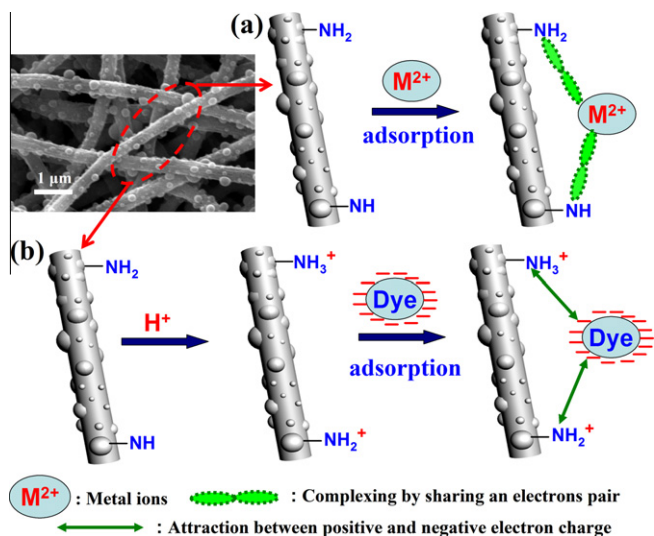


Fig. 14. Typical XPS wide scan spectra for the micro-nano structure PES/PEI nanofibrous membrane: before adsorption (a); Cu adsorbed (b); Pb adsorbed (c); Cd adsorbed (d); SY FCF adsorbed (e); GF FCF adsorbed (f); and AM adsorbed (g). The inset shows the characteristic peaks of N 1s and metal ions with higher resolution.



**Fig. 15.** Possible adsorption mechanism for heavy metal ions (a) and anionic dyes (b) with bifunctional amino and imino groups on the micro-nano structure PES/PEI nanofibrous membranes.

**Table 5**

Desorption efficiency of the anionic dyes and heavy metal ions on PES/PEI nanofibrous membranes from three adsorption–desorption cycles.

Recycle times	Desorption percentage (%)					
	SY FCF	FG FCF	AM	Pb(II)	Cu(II)	Cd(II)
1	99.8	90.6	72.2	99.5	99.3	99.6
2	99.5	89.2	70.4	99.2	98.6	97.6
3	96.0	88.6	70.6	96.2	98.2	97.2

at relatively high level, but desorption efficiency of AM was lowered to 70.6%, and the reason was not clear till now. These data were comparable to those using NaOH as regeneration solution [1] and higher than those using ethanol [55] or surfactant [56] as solvent for desorption. In a word, these results indicated that EDTA and NaOH were useful desorption agents for recovering PES/PEI nanofibrous membrane used for removal of heavy metal ions and anionic dyes, respectively.

#### 4. Conclusion

In this study, a novel micro-nano structure PES/PEI nanofibrous membrane was used as an adsorbent for anionic dyes and cationic metal ions depending on the pH value of the aqueous solution. It was found that the optimum solution pH for the adsorption of heavy metal ions and anionic dyes was 5–7 and 1, respectively. The adsorption behavior of heavy metal ions and anionic dyes on PES/PEI nanofibrous membrane can be well fitted with the Langmuir adsorption isotherm, and the maximum adsorption capacity of SY FCF, FG FCF, AM, Pb(II), Cu(II) and Cd(II) were 1000.00 mg/g, 344.83 mg/g, 454.44 mg/g, 94.34 mg/g, 161.29 mg/g and 357.14 mg/g, respectively. Thermodynamic parameters were calculated using the van't Hoff equation. The results indicated that the adsorption process for anionic dyes was different as that for heavy metal ions. It was found that the adsorption of anionic dyes on PES/PEI nanofibrous membrane was endothermic, whereas, the adsorption of heavy metal ions on PES/PEI nanofibrous membrane was exothermic. Furthermore, the adsorption for both anionic dyes and heavy metal ions was spontaneous and physical adsorption. The micro-nano structure PES/PEI membrane could be regenerated

successfully in suitable solutions. Since amino group was one of the most efficient functional groups used in affinity application, the results of this study will be beneficial to the development of amino-group-containing adsorbents for the removal of anionic and cationic compounds from aqueous solution.

#### Acknowledgments

This work was supported by National Science Foundation of China (20874009 and 21174028), Innovation Program of Shanghai Municipal Education Commission, National Science Foundation of China for Distinguished Young Scholars (50925312), Fundamental Research Funds for the Central Universities and 111 Project (111-2-04).

#### References

- Y.F. Lin, H.W. Chen, P.S. Chien, C.S. Chiou, C.C. Liu, Application of bifunctional magnetic adsorbent to adsorb metal cations and anionic dyes in aqueous solution, *J. Hazard. Mater.* 185 (2011) 1124–1130.
- C.H. Huang, K.P. Chang, H.D. Ou, Y.C. Chiang, C.F. Wang, Adsorption of cationic dyes onto mesoporous silica, *Microporous Mesoporous Mater.* 141 (2011) 102–109.
- M.U. Dural, L. Cavas, S.K. Papageorgiou, F.K. Katsaros, Methylene blue adsorption on activated carbon prepared from *Posidonia oceanica* (L.) dead leaves: kinetics and equilibrium studies, *Chem. Eng. J.* 168 (2011) 77–85.
- S. Xiao, M. Shen, R. Guo, Q. Huang, S. Wang, X. Shi, Fabrication of multiwalled carbon nanotube-reinforced electrospun polymer nanofibers containing zero-valent iron nanoparticles for environmental applications, *J. Mater. Chem.* 20 (2010) 5700–5708.
- D. Wesenberg, I. Kyriakides, S.N. Agathos, White-rot fungi and their enzymes for the treatment of industrial dye effluents, *Biotechnol. Adv.* 22 (2003) 161–187.
- C.S. Ki, E.H. Gang, I.C. Um, Y.H. Park, Nanofibrous membrane of wool keratose/silk fibroin blend for heavy metal ion adsorption, *J. Membr. Sci.* 302 (2007) 20–26.
- K. Yoshimatsu, L. Ye, J. Lindberg, I.S. Chronakis, Selective molecular adsorption using electrospun nanofiber affinity membranes, *Biosens. Bioelectron.* 23 (2008) 1208–1215.
- Z. Ma, Z. Lan, T. Matsuura, S. Ramakrishna, Electrospun polyethersulfone affinity membrane: membrane preparation and performance evaluation, *J. Chromatogr. B* 877 (2009) 3686–3694.
- Z. Ma, M. Kotaki, S. Ramakrishna, Electrospun cellulose nanofiber as affinity membrane, *J. Membr. Sci.* 265 (2005) 115–123.
- D.H. Reneker, I. Chun, Nanometer diameter fibers of polymer, produced by electrospinning, *Nanotechnology* 7 (1996) 216–223.
- H. Fong, I. Chun, D.H. Reneker, Beaded nanofibers formed during electrospinning, *Polymer* 40 (1999) 4585–4592.
- C.C. Liu, M.K. Wang, Y.S. Li, Removal of nickel from aqueous solution using wine processing waste sludge, *Ind. Eng. Chem. Res.* 44 (2005) 1438–1445.
- N. Li, R.B. Bai, C. Liu, Enhanced and selective adsorption of mercury ions on chitosan beads grafted with polyacrylamide via surface-initiated atom transfer radical polymerization, *Langmuir* 21 (2005) 11780–11787.
- N. Li, R.B. Bai, Copper adsorption on chitosan–cellulose hydrogel beads: behaviors and mechanisms, *Sep. Purif. Technol.* 42 (2005) 237–247.
- M. Ghoul, M. Bacquet, M. Morcellet, Uptake of heavy metals from synthetic aqueous solutions using modified PEI-silica gels, *Water Res.* 37 (2003) 729–734.
- R.K. Gupta, R.A. Singh, S.S. Dubey, Removal of mercury ions from aqueous solutions by composite of polyaniline with polystyrene, *Sep. Purif. Technol.* 38 (2004) 225–232.
- C.S. Chiou, J.S. Shih, Bifunctional cryptand modifier for capillary electrophoresis in separation of inorganic/organic anions and inorganic cations, *Analyst* 121 (1996) 1107–1110.
- S. Babacan, P. Pivarnik, S. Letcher, A. Rand, Evaluation of antibody immobilization methods for piezoelectric biosensor application, *Biosens. Bioelectron.* 15 (2000) 615–621.
- R. Bunde, E. Jarvi, J. Rosentreter, A piezoelectric method for monitoring formaldehyde induced crosslink formation between poly-L-lysine and poly-deoxyguanosine, *Talanta* 51 (2000) 159–171.
- M. Kikuchi, S. Shiratori, Quartz crystal microbalance (QCM) sensor for  $\text{CH}_3\text{SH}$  gas by using polyelectrolyte-coated sol–gel film, *Sens. Actuat. B* 108 (2005) 564–571.
- X. Wang, B. Ding, M. Sun, J. Yu, G. Sun, Nanofibrous polyethyleneimine membranes as sensitive coatings for quartz crystal microbalance-based formaldehyde sensors, *Sens. Actuat. B* 144 (2010) 11–17.
- X. Wang, M. Min, Z. Liu, Y. Yang, Z. Zhou, M. Zhu, Y. Chen, B.S. Hsiao, Poly(ethyleneimine) nanofibrous affinity membrane fabricated via one step wet-electrospinning from poly(vinyl alcohol)-doped poly(ethyleneimine) solution system and its application, *J. Membr. Sci.* 379 (2011) 191–199.



- [23] L. Lebrun, F. Vallee, B. Alexandre, Q.T. Nguyen, Preparation of chelating membranes to remove metal cations from aqueous solutions, *Desalination* 207 (2007) 9–23.
- [24] B.L. Rivas, E.D. Pereira, I. Moreno-Villoslada, Water-soluble polymer-metal ion interactions, *Prog. Polym. Sci.* 28 (2003) 173–208.
- [25] H. Bessbousse, T. Rhilalou, J.F. Verchere, L. Lebrun, Removal of heavy metal ions from aqueous solutions by filtration with a novel complexing membrane containing poly(ethyleneimine) in a poly(vinyl alcohol) matrix, *J. Membr. Sci.* 307 (2008) 249–259.
- [26] M. Min, X. Wang, Y. Yang, Z. Liu, Z. Zhou, M. Zhu, Y. Chen, B.S. Hsiao, Fabrication of micro-nano structure nanofibers by solvent etching, *J. Nanosci. Nanotechnol.* 11 (2011) 6919–6925.
- [27] J.H. Hong, M.C. Park, S.K. Hong, B.S. Kim, Preparation of an anion-exchange membrane by the amination of chlorinated polypropylene and polyethyleneimine at a low temperature and its ion-exchange property, *J. Appl. Polym. Sci.* 112 (2009) 830–835.
- [28] N. Saxena, C. Prabhavathy, S. De, S. DasGupta, Flux enhancement by argon-oxygen plasma treatment of polyethersulfone membranes, *Sep. Purif. Technol.* 70 (2009) 160–165.
- [29] K.H. Wu, P.Y. Yu, Y.J. Hsieh, C.C. Yang, G.P. Wang, Preparation and characterization of silver-modified poly(vinyl alcohol)/polyethyleneimine hybrids as a chemical and biological protective material, *Polym. Degrad. Stab.* 94 (2009) 2170–2177.
- [30] W. Cui, J. Kerres, G. Eigenberger, Development and characterization of ion-exchange polymer blend membranes, *Sep. Purif. Technol.* 14 (1998) 145–154.
- [31] A. Saleem, L. Frommann, A. Iqbal, High performance thermoplastic composites: study on the mechanical, thermal, and electrical resistivity properties of carbon fiber-reinforced polyetheretherketone and polyethersulphone, *Polym. Compos.* 28 (2007) 785–796.
- [32] R. Liang, H. Cao, D. Qian, MoO<sub>3</sub> nanowires as electrochemical pseudocapacitor materials, *Chem. Commun.* 47 (2011) 10305–10307.
- [33] F. Zhao, X. Wang, B. Ding, J. Lin, J. Hu, Y. Si, J. Yu, G. Sun, Nanoparticle decorated fibrous silica membranes exhibiting biomimetic superhydrophobicity and highly flexible properties, *RSC Adv.* 1 (2011) 1482–1488.
- [34] D. Sun, X. Zhang, Y. Wu, X. Liu, Adsorption of anionic dyes from aqueous solution on fly ash, *J. Hazard. Mater.* 181 (2010) 335–342.
- [35] G. Annadurai, L.Y. Ling, J.F. Lee, Adsorption of reactive dye from an aqueous solution by chitosan: isotherm, kinetic and thermodynamic analysis, *J. Hazard. Mater.* 152 (2008) 337–346.
- [36] S.Y. Chen, Y. Zou, Z.Y. Yan, W. Shen, S.K. Shi, X. Zhang, H.P. Wang, Carboxymethylated-bacterial cellulose for copper and lead ion removal, *J. Hazard. Mater.* 161 (2009) 1355–1359.
- [37] M.S. Chiou, H.Y. Li, Equilibrium and kinetic modeling of adsorption of reactive dye on cross-linked chitosan beads, *J. Hazard. Mater.* 93 (2002) 233–248.
- [38] S. Chen, W. Shen, F. Yu, H. Wang, Kinetic and thermodynamic studies of adsorption of Cu<sup>2+</sup> and Pb<sup>2+</sup> onto amidoximated bacterial cellulose, *Polym. Bull.* 63 (2009) 283–297.
- [39] A. El-Sikaily, A.E. Nembr, A. Khaled, O. Abdelwehab, Removal of toxic chromium from wastewater using green alga *ulva lactuca* and its activated carbon, *J. Hazard. Mater.* 148 (2007) 216–228.
- [40] H.M.F. Freundlich, Over the adsorption in solution, *J. Phys. Chem.* 57 (1906) 385–470.
- [41] A. Mellah, S. Chegrouche, M. Barkat, The removal of uranium(VI) from aqueous solutions onto activated carbon: kinetic and thermodynamic investigations, *J. Colloid Interf. Sci.* 296 (2006) 434–441.
- [42] Y.S. Ho, G. McKay, Sorption of dye from aqueous solution by peat, *Chem. Eng. J.* 70 (1998) 115–124.
- [43] C. Cheng, L. Ma, J. Ren, L. Li, G. Zhang, Q. Yang, C. Zhao, Preparation of polyethersulfone-modified sepiolite hybrid particles for the removal of environmental toxins, *Chem. Eng. J.* 171 (2011) 1132–1142.
- [44] F.C. Wu, R.L. Tseng, R.S. Juang, Initial behavior of intraparticle diffusion model used in the description of adsorption kinetics, *Chem. Eng. J.* 153 (2009) 1–8.
- [45] J. Wang, L. Xua, Y. Meng, C. Cheng, A. Li, Adsorption of Cu<sup>2+</sup> on new hyper-crosslinked polystyrene adsorbent: batch and column studies, *Chem. Eur. J.* 178 (2011) 108–114.
- [46] X.Y. Huang, J.P. Bin, H.T. Bu, G.B. Jiang, M.H. Zeng, Removal of anionic dye eosin Y from aqueous solution using ethylenediamine modified chitosan, *Carbohydr. Polym.* 84 (2011) 1350–1356.
- [47] A. Rodriguez, G. Ovejero, M. Mestanza, J. Garcia, Removal of dyes from wastewaters by adsorption on sepiolite and pansil, *Ind. Eng. Chem. Res.* 49 (2010) 3207–3216.
- [48] N. Mohammadi, H. Khani, V.K. Gupta, E. Amereh, S. Agarwal, Adsorption process of methyl orange dye onto mesoporous carbon material-kinetic and thermodynamic studies, *J. Colloid Interf. Sci.* 362 (2011) 457–462.
- [49] J. Meng, J. Yuan, Y. Kang, Y. Zhang, Q. Du, Surface glycosylation of polysulfone membrane towards a novel complexing membrane for boron removal, *J. Colloid Interf. Sci.* 368 (2012) 197–207.
- [50] H. Yan, J. Dai, Z. Yang, H. Yang, R. Cheng, Enhanced and selective adsorption of copper(II) ions on surface carboxymethylated chitosan hydrogel beads, *Chem. Eng. J.* 174 (2011) 586–594.
- [51] C. Shen, Y. Wen, X. Kang, W. Liu, H<sub>2</sub>O<sub>2</sub>-induced surface modification: a facile, effective and environmentally friendly pretreatment of chitosan for dyes removal, *Chem. Eng. J.* 166 (2011) 474–482.
- [52] Q. Chen, D. Yin, S. Zhu, X. Hua, Adsorption of cadmium(II) on humic acid coated titanium dioxide, *J. Colloid Interf. Sci.* 367 (2012) 241–248.
- [53] X.G. Li, H. Feng, M.R. Huang, Redox sorption and recovery of silver ions as silver nanocrystals on poly(aniline-co-5-sulfo-2-anisidine) nanosorbents, *Chem. Eur. J.* 16 (2010) 10113–10123.
- [54] Q.F. Lu, X.G. Li, M.R. Huang, Synthesis and heavy-metal-ion sorption of pure sulfophenylenediamine copolymer nanoparticles with intrinsic conductivity and stability, *Chem. Eur. J.* 13 (2007) 6009–6018.
- [55] W. Tanthapanichakoon, P. Ariyadejwanich, P. Japthong, K. Nakagawa, S.R. Mukai, H. Tamon, Adsorption-desorption characteristics of phenol and reactive dyes from aqueous solution on mesoporous activated carbon prepared from waste tires, *Water Res.* 39 (2005) 1347–1353.
- [56] M.K. Purkait, S. DasGupta, S. De, Adsorption of eosin dye on activated carbon and its surfactant based desorption, *J. Environ. Manage.* 76 (2005) 135–142.